Forcible destruction of severely misfolded mammalian glycoproteins by the non-glycoprotein ERAD pathway.

AUTHOR(S):

Ninagawa, Satoshi; Okada, Tetsuya; Sumitomo, Yoshiki; Horimoto, Satoshi; Sugimoto, Takehiro; Ishikawa, Tokiro; Takeda, Shunichi; ... Kamiya, Yukiko; Kato, Koichi; Mori, Kazutoshi

CITATION:

Ninagawa, Satoshi ...[et al]. Forcible destruction of severely misfolded mammalian glycoproteins by the non-glycoprotein ERAD pathway.. The Journal of cell biology 2015, 211(4): 775-784

ISSUE DATE:

2015-11-16

URL:

http://hdl.handle.net/2433/201885

Forcible destruction of severely misfolded mammalian glycoproteins by the non-glycoprotein ERAD pathway

Satoshi Ninagawa,[1,3,4] Tetsuya Okada,[1] Yoshiki Sumitomo,[1] Satoshi Horimoto,[1] Takehiro Sugimoto,[1] Tokiro Ishikawa,[1] Shunichi Takeda,[2] Takashi Yamamoto,[5] Tadashi Suzuki,[6] Yukiko Kamiya,[3,4] Koichi Kato,[3,4,7] and Kazutoshi Mori[1]

[1]Department of Biophysics, Graduate School of Science, Kyoto University, Sakyo-ku, Kyoto 606-8502, Japan
[2]Department of Radiation Genetics, Graduate School of Medicine, Kyoto University, Sakyo-ku, Kyoto 606-8501, Japan
[3]Institute for Molecular Science and [4]Okazaki Institute for Integrative Bioscience, National Institutes of Natural Sciences, Myodaiji, Okazaki 444-8787, Japan
[5]Department of Mathematical and Life Sciences, Graduate School of Science, Hiroshima University, Higashi-Hiroshima 739-8526, Japan
[6]Glycometabolome Team, Systems Glycobiology Research Group, RIKEN Global Research Cluster, Wako, Saitama 351-0198, Japan
[7]Graduate School of Pharmaceutical Sciences, Nagoya City University, Mizuho-ku, Nagoya, 467-8603, Japan

Glycoproteins and non-glycoproteins possessing unfolded/misfolded parts in their luminal regions are cleared from the endoplasmic reticulum (ER) by ER-associated degradation (ERAD)-L with distinct mechanisms. Two-step mannose trimming from $Man_9GlcNAc_2$ is crucial in the ERAD-L of glycoproteins. We recently showed that this process is initiated by EDEM2 and completed by EDEM3/EDEM1. Here, we constructed chicken and human cells simultaneously deficient in EDEM1/2/3 and analyzed the fates of four ERAD-L substrates containing three potential N-glycosylation sites. We found that native but unstable or somewhat unfolded glycoproteins, such as ATF6α, ATF6α(C), CD3-δ–ΔTM, and EMC1, were stabilized in EDEM1/2/3 triple knockout cells. In marked contrast, degradation of severely misfolded glycoproteins, such as null Hong Kong (NHK) and deletion or insertion mutants of ATF6α(C), CD3-δ–ΔTM, and EMC1, was delayed only at early chase periods, but they were eventually degraded as in wild-type cells. Thus, higher eukaryotes are able to extract severely misfolded glycoproteins from glycoprotein ERAD and target them to the non-glycoprotein ERAD pathway to maintain the homeostasis of the ER.

Introduction

Soluble or transmembrane proteins in the ER possessing unfolded or misfolded parts in their luminal regions are retrotranslocated back to the cytoplasm and degraded by the proteasome, a series of events termed ER-associated degradation (ERAD)-L (Xie and Ng, 2010; Smith et al., 2011; Brodsky, 2012).

ERAD-L deals with both glycoproteins (gpERAD) and non-glycoproteins (non-gpERAD). Misfolded parts of non-glycoproteins are most likely recognized by molecular chaperones represented by BiP. In contrast, glycoprotein degradation relies on the structure of N-glycans present on the surface of ERAD-L substrates. $Glc_3Man_9GlcNAc_2$ attached to the asparagine residue is trimmed by glucosidase I and II to $Man_9GlcNAc_2$, which is in turn trimmed to $Man_8GlcNAc_2$ and then to $Man_7GlcNAc_2$. $Man_7GlcNAc_2$ exposing α1,6-linked mannose is recognized by the lectin molecule for the delivery of ERAD-L substrates to the HRD1 E3 complex present in the ER membrane (Molinari, 2007; Hosokawa et al., 2010; Kamiya et al., 2012).

We have recently conducted comprehensive gene knockout (KO) analyses to precisely identify the roles of the four α1,2-mannosidase candidates for the mannose trimming that occurs during ERAD-L, namely ER mannosidase I (ERmanI), EDEM1, EDEM2, and EDEM3. These experiments were performed in chicken DT40 cells using conventional homologous recombination and in human HCT116 cells using the transcription activator-like effector nuclease method. Our results were surprising (Ninagawa et al., 2014). Initial trimming from $Man_9GlcNAc_2$ to $Man_8GlcNAc_2$ was conducted by EDEM2, which had been thought to have no mannosidase activity (Mast et al., 2005), whereas subsequent trimming from $Man_8GlcNAc_2$ to $Man_7GlcNAc_2$ was performed mostly by EDEM3 and to a slight extent by EDEM1. ERmanI appeared to play only a minor role in gpERAD.

Here, by constructing and analyzing DT40 and HCT116 cells simultaneously deficient in EDEM1/2/3, we show that different ERAD pathways are used depending on the severity of

Correspondence to Koichi Kato: kkato@phar.nagoya-cu.ac.jp; or Kazutoshi Mori: mori@upr.biophys.kyoto-u.ac.jp

Y. Kamiya's present address is Graduate School of Engineering and EcoTopia Science Institute, Nagoya University, Chikusa-ku, Nagoya 464-8603, Japan.

Abbreviations used in this paper: α1PI, α1-proteinase inhibitor; EndoH, endoglycosidase H; ERAD, ER-associated degradation; ERmanI, ER mannosidase I; KO, knockout; MEF, mouse embryonic fibroblast; NHK, null Hong Kong; PNGase, peptide:N-glycanase; PQQ, pyrroloquinoline quinone; TKO, triple KO; WT, wild type.

Supplemental Material can be found at:
http://jcb.rupress.org/content/suppl/2015/11/04/jcb.201504109.DC1.html
Original image data can be found at:
http://jcb-dataviewer.rupress.org/jcb/browse/10702

The Rockefeller University Press $30.00
J. Cell Biol. Vol. 211 No. 4 775–784
www.jcb.org/cgi/doi/10.1083/jcb.201504109

misfolding in the ERAD-L substrates and that non-gpERAD has a much more positive role in protein quality control in the ER than its previously proposed role as a backup for gpERAD under ER stress (Ushioda et al., 2013), as indicated by the finding that non-gpERAD is able to clear severely misfolded glycoproteins from the ER even in the absence of pharmacological ER stress.

Results and discussion

We constructed EDEM1/2/3 triple KO (TKO) in both DT40 (gEDEM-TKO; Fig. S1) and HCT116 (hEDEM-TKO; Fig. S2 A) cells, in which functional EDEM1, EDEM2, or EDEM3 mRNA was not expressed (Fig. 1, A and C). gEDEM-TKO and hEDEM-TKO cells grew slightly more slowly than respective wild-type (WT) cells (Fig. 1, A and C). However, ER stress was not elicited in these cells because the levels of three ER stress marker proteins, BiP, ATF4, and XBP1(S), were not elevated (Fig. S2 B). The N-glycan profiles of total cellular glycoproteins revealed that M9 level was markedly elevated in gEDEM-TKO and hEDEM-TKO cells, similarly to WT DT40 and HCT116 cells treated with kifunensine, an inhibitor of α1,2-mannosidases in the ER (Fig. 1, B and D), as expected from our previous results (Ninagawa et al., 2014). Accordingly, degradation of endogenous ATF6α, an ERAD-Lm (m for membrane protein) substrate containing three potential N-glycosylation sites (Fig. 3 A) was blocked almost completely in gEDEM-TKO and hEDEM-TKO cells (Fig. 1, E and F). The extent of this blockade was comparable with that observed in WT cells treated with MG132, a proteasome inhibitor, or kifunensine (Ninagawa et al., 2014). We also found that hATF6α(C)-TAP, an artificial ERAD-Ls (s for soluble protein) substrate containing the luminal region of human ATF6α flanked by the N-terminal signal sequence and C-terminal tandem affinity purification tag (Fig. 3 A), was stabilized in gEDEM-TKO cells (Fig. 1 G). During SDS-PAGE, hATF6α(C)-TAP in gEDEM-TKO cells migrated slightly more slowly than in WT cells because of the defect in mannose trimming, and this difference in migration was lost after endoglycosidase H (EndoH) treatment (Fig. 1 H). Instability of the native protein ATF6α in WT cells may result from intrinsically disordered parts found in its luminal region (Rosenbaum et al., 2011).

We next examined the effect of EDEM-TKO on degradation of the null Hong Kong (NHK) variant of α1-proteinase inhibitor (α1PI), the most frequently used ERAD-Ls substrate (Sifers et al., 1988). Similarly to the case of hATF6α(C)-TAP, NHK in gEDEM-TKO cells migrated slightly more slowly than in WT cells during SDS-PAGE, and this difference in migration was lost after EndoH treatment (Fig. 2 A). In the case of NHK-QQQ, the nonglycosylated version of NHK and its migration positions during SDS-PAGE (Fig. 2 A), as well as its degradation rate (Fig. 2 B), did not differ between WT and gEDEM-TKO cells, as expected. However, in marked contrast to the case of ATF6α (Ninagawa et al., 2014), we were surprised to find that NHK was degraded similarly in WT and gEDEM1/2/3 single KO (Fig. 2 C) and in WT and hEDEM1/2/3 single KO cells (Fig. 2 F). Furthermore, degradation of NHK was delayed only at early chase periods in gEDEM-TKO (Fig. 2 D) and hEDEM-TKO (Fig. 2 G) cells, and NHK was eventually degraded in gEDEM-TKO and hEDEM-TKO cells similarly to the case in WT cells. This delay in early chase period was also observed in WT DT40 (Fig. 2 E) and HCT116 (Fig. 2, G and H) cells treated with kifunensine, whereas NHK degradation was significantly delayed at all chase periods in WT DT40 (Fig. 2 E) and HCT116 (Fig. 2 H) cells treated with MG132. Kifunensine treatment of hEDEM-TKO cells did not affect the degradation rate of NHK, as expected (Fig. 2 G). Thus, the fates of ERAD-L substrates in cells defective in mannose trimming differ depending on the substrate examined.

We hypothesized that chicken and human cells are able to extract severely misfolded glycoproteins, such as NHK containing C-terminal large truncation, from gpERAD and target them to non-gpERAD, which degrades substrates such as NHK-QQQ (Fig. 2 B). To probe this hypothesis, we introduced various deletions into hATF6α(C)-TAP to exacerbate its degree of misfolding. At the same time, we removed the 2×IgG binding domain from hATF6α(C)-TAP to make hATF6α(C)-myct, on the basis that the presence of such a folded domain may obscure the effect of deletion on the folding status of hATF6α(C) (Fig. 3 A). This hATF6α(C)-myct was markedly stabilized in gEDEM-TKO cells (Fig. 3 C). We then constructed its three deletion mutants (Fig. 3 A). All four proteins entered the ER and became glycosylated, as they migrated slightly more slowly in gEDEM-TKO cells than in WT cells during SDS-PAGE, and the difference in migration was lost after EndoH treatment (Fig. 3 B). Cycloheximide chase experiments revealed that the deletion of aa 280–298 did not significantly affect the stability of hATF6α(C)-myct (Fig. 3 D). In contrast, the Δ111–119, 182–194 mutant and Δ219–270 mutant became very unstable in gEDEM-TKO cells and behaved very similarly to NHK; their degradation was delayed only at the early chase periods in gEDEM-TKO cells, and they were eventually degraded in both WT and gEDEM-TKO cells (Fig. 3, E and F). It should be noted that degradation of all four glycoproteins was blocked by MG132 treatment in both WT and gEDEM-TKO cells (Fig. S2 C).

To determine whether the folding status of the four glycoproteins is correlated with their fates in gEDEM-TKO cells, we used several approaches. It was previously shown that a denatured glycoprotein is more susceptible to mannose trimming by ERmanI than a native protein (Aikawa et al., 2012). In this connection, we noticed that when cells were lysed directly in SDS sample buffer, hATF6α(C)-myct1-302 and the Δ280–298 mutant were detected as a single band, whereas the Δ111–119, 182–194 and Δ219–270 mutants were detected as a doublet, although slower bands were predominant (Fig. S3 A). When cells were lysed with digitonin and then mixed with 2× SDS sample buffer, faster bands of hATF6α(C)-myct1-302 and the Δ280–298 mutant appeared, and levels of faster bands of the Δ111–119, 182–194 and Δ219–270 mutants increased (Fig. S3 A). We interpret this appearance of faster bands upon lysis with digitonin to represent partial deglycosylation of hATF6α(C) derivatives by peptide:N-glycanase (PNGase), an enzyme responsible for deglycosylation of glycoproteins dislocated from the ER to the cytosol (Misaghi et al., 2004), for three reasons. First, both bands were sensitive to EndoH treatment (Fig. S3 B); second, the appearance of the faster band of the Δ111–119, 182–194 mutant was significantly inhibited by Z-VAD-fmk (Fig. S3 C), which inhibits PNGase; and third, the faster band of the Δ111–119, 182–194 mutant did not appear in mouse embryonic fibroblast (MEF) cells deficient in PNGase but did appear in MEF cells deficient in the cytosolic endo-β-*N*-acetylglucosaminidase (ENGase; Fig. S3 D; Huang et al., 2015). The time course of the appearance

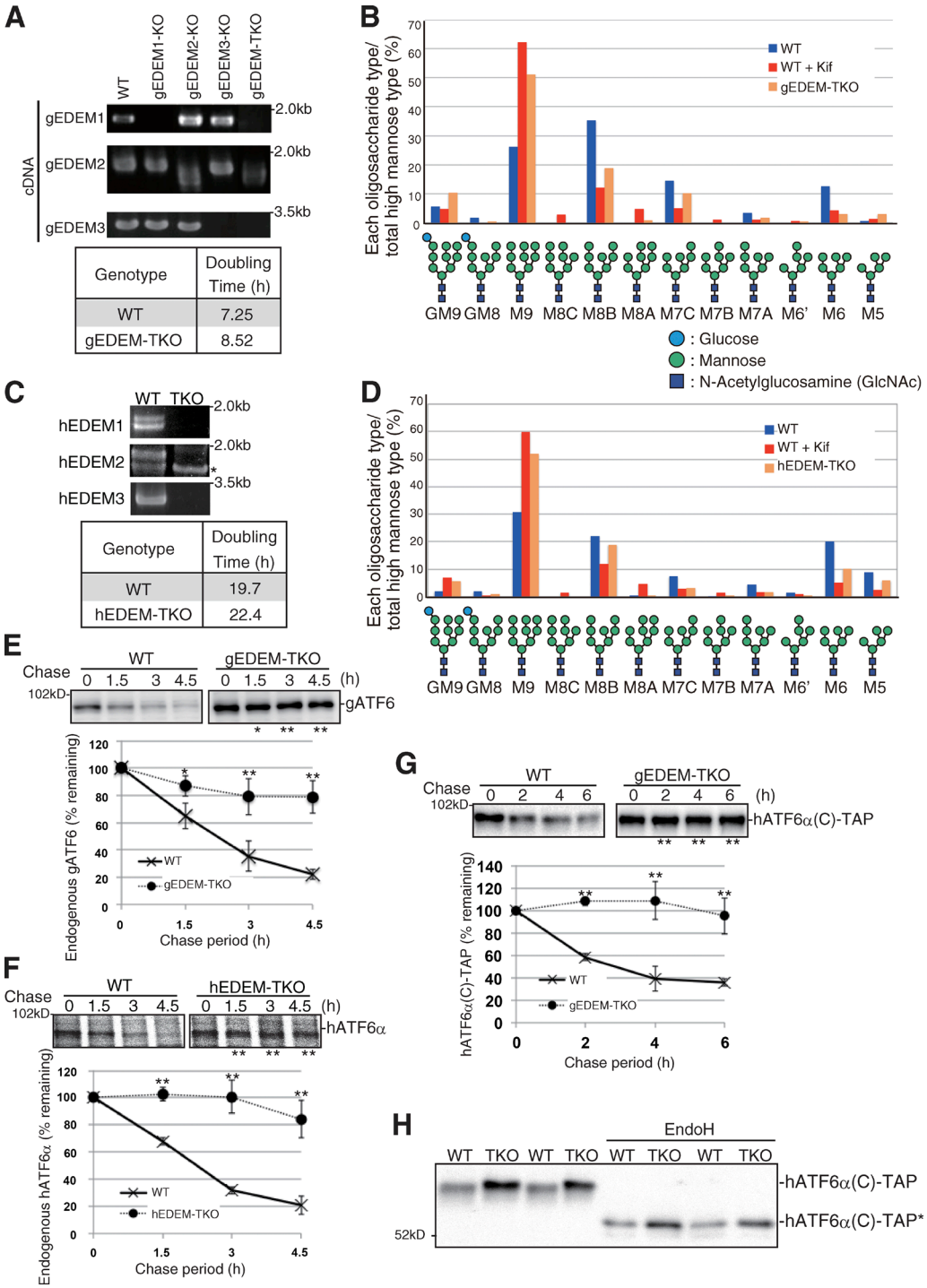

Figure 1. **Effect of EDEM-TKO on N-glycan profiles and ATF6α degradation.** (A) RT-PCR to amplify cDNA corresponding to gEDEM1/2/3 mRNA in DT40 cells of various genotypes and doubling times of WT and gEDEM-TKO cells. (B) Isomer composition of N-glycans prepared from total cellular glycoproteins of WT, WT treated with kifunensine (Kif, 10 μg/ml, 6 h), and gEDEM-TKO cells. This experiment was completed once. (C) RT-PCR to amplify cDNA corresponding to hEDEM1/2/3 mRNA in WT and hEDEM-TKO cells and their doubling times. The asterisk denotes a nonspecific band. (D) Isomer composition of N-glycans prepared from total cellular glycoproteins of WT, WT treated with kifunensine (10 μg/ml, 12 h), and hEDEM-TKO cells. This experiment was completed once. (E) Cycloheximide chase to determine the degradation rate of endogenous gATF6 (only one *ATF6* gene in chicken genome) in WT and gEDEM-TKO cells using anti-gATF6 ($n = 3$). (F) Pulse-chase to determine the degradation rate of endogenous hATF6α in WT and hEDEM-TKO cells using anti-hATF6α ($n = 3$). (G) Cycloheximide chase to determine the degradation rate of transfected hATF6α(C)-TAP in WT and gEDEM-TKO cells using anti–c-myc ($n = 3$). (E–G) Means ± SD are shown. *, $P < 0.05$; **, $P < 0.01$. (H) Immunoblotting of cell lysates prepared from WT and gEDEM-TKO cells expressing transfected hATF6α(C)-TAP with or without EndoH treatment using anti–c-myc. hATF6α(C)-TAP* denotes the nonglycosylated hATF6α(C)-TAP.

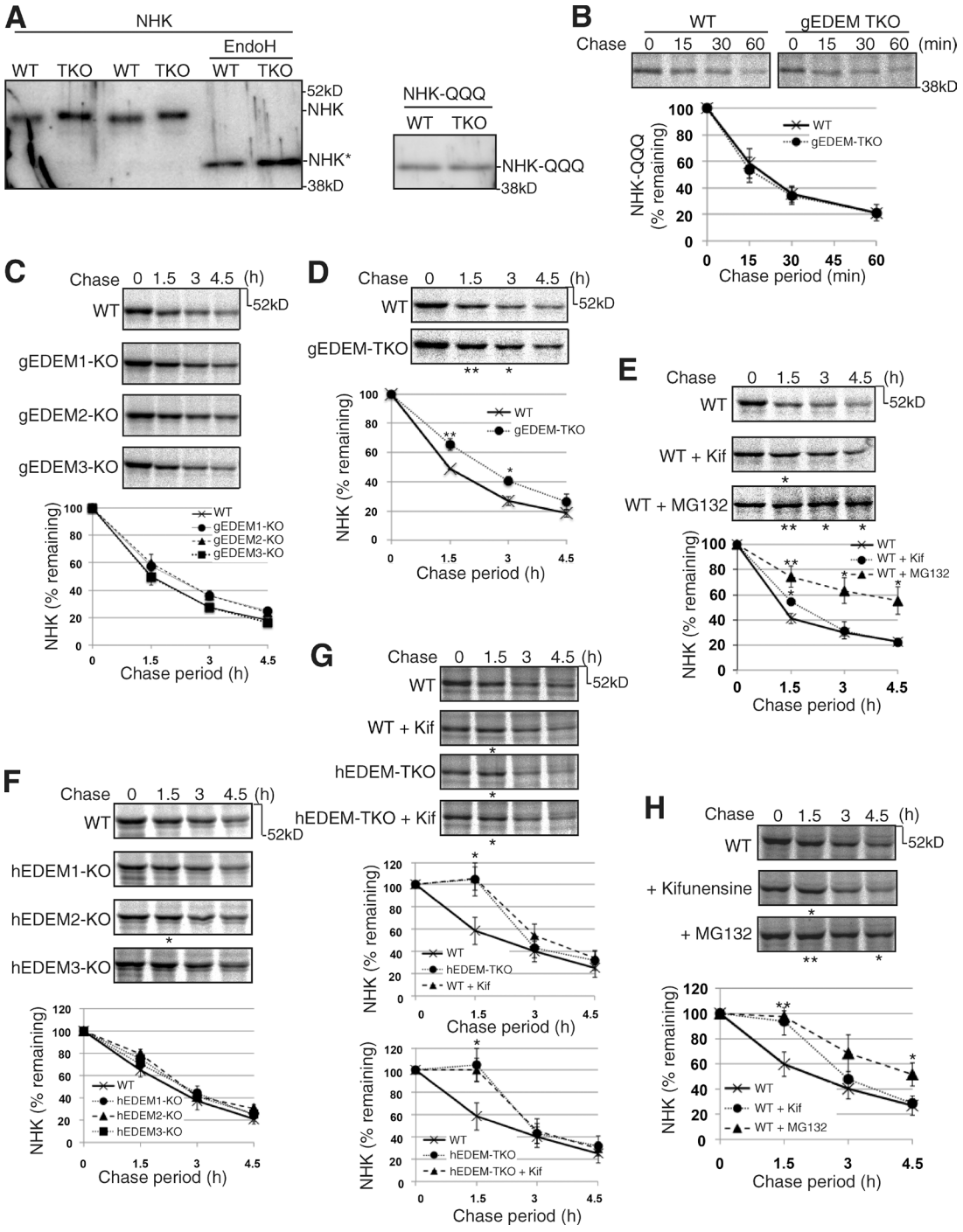

Figure 2. **Effect of EDEM-TKO on NHK degradation.** (A) Immunoblotting of cell lysates prepared from WT and gEDEM-TKO cells expressing transfected NHK with or without EndoH treatment and those expressing transfected NHK-QQQ, using anti-α1PI. NHK* denotes the nonglycosylated NHK. (B) Pulse-chase to determine the degradation rate of transfected NHK-QQQ in WT and gEDEM-TKO cells using anti-α1PI (n = 3). (C) Pulse-chase to determine the degradation rate of transfected NHK in WT and gEDEM1/2/3 single KO cells using anti-α1PI (n = 3). (D) Pulse-chase to determine the degradation rate of transfected NHK in WT and gEDEM-TKO cells using anti-α1PI (n = 3). (E) Pulse-chase to determine the degradation rate of transfected NHK in WT DT40 cells and those treated with kifunensine (10 µg/ml) or MG132 (30 µM) using anti-α1PI (n = 3). (F) Pulse-chase to determine the degradation rate of transfected NHK in WT and hEDEM1/2/3 single KO cells using anti-α1PI (n = 3). (G) Pulse-chase to determine the degradation rate of transfected NHK in WT and hEDEM-TKO cells in the presence or absence of kifunensine (10 µg/ml) using anti-α1PI (n = 3). (H) Pulse-chase to determine the degradation rate of transfected NHK in WT HCT116 cells and those treated with kifunensine (10 µg/ml) or MG132 (20 µM) using anti-α1PI (n = 3). (B–H) Means ± SD are shown. (D–H) *, $P < 0.05$; **, $P < 0.01$.

of faster bands in PNGase sensitivity assay in cell lysates indicated that the Δ111–119, 182–194 and Δ219–270 mutants were more misfolded than hATF6α(C)-myct1-302 and the Δ280–298 mutant (Fig. S3 E).

It was also previously reported that a misfolded protein is more susceptible to trypsin digestion than a folded protein (Izawa et al., 2012; Xu et al., 2013). The results of trypsin sensitivity assay suggested that the Δ111–119, 182–194 and Δ219–270

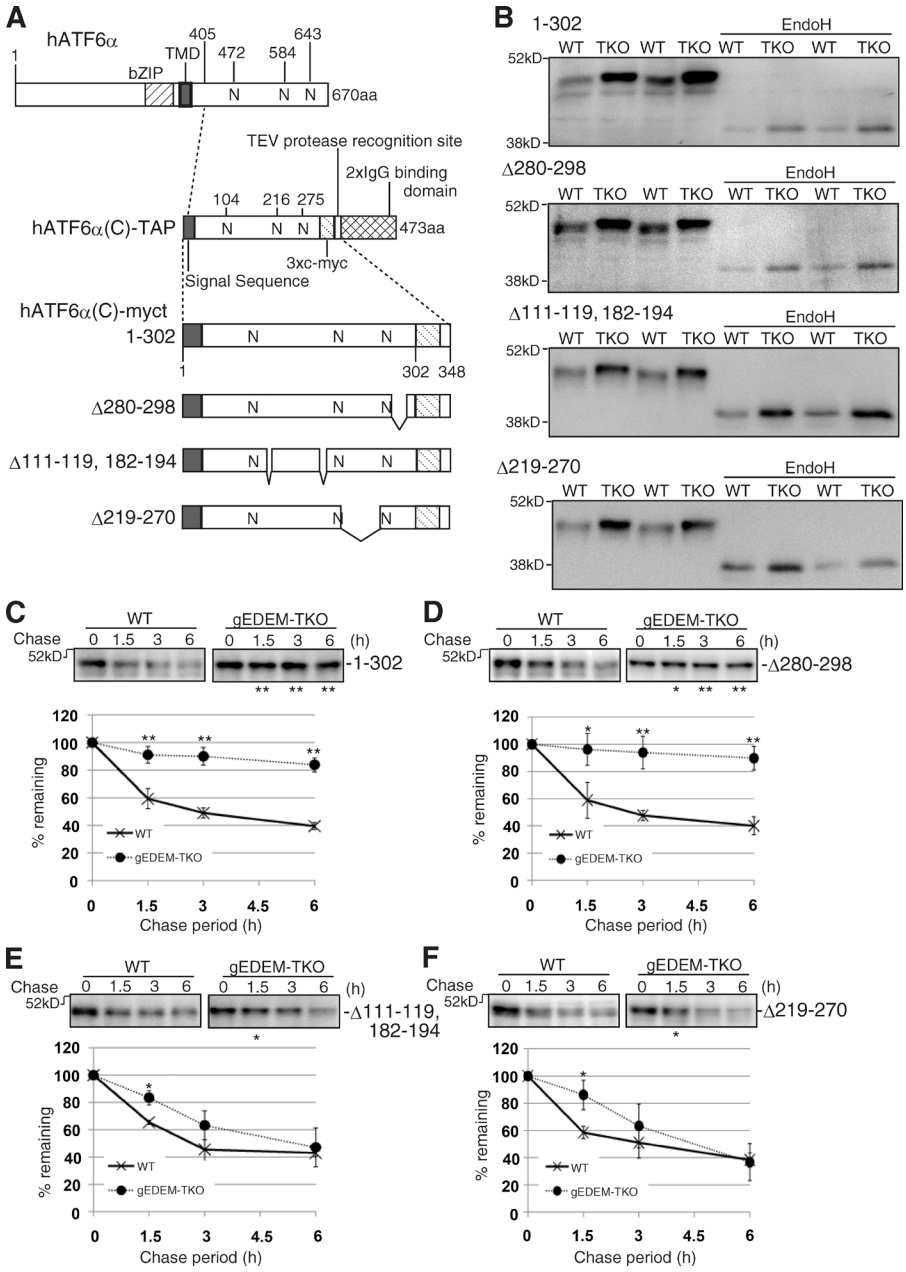

Figure 3. **Effect of EDEM-TKO on hATF6α(C)-myct degradation.** (A) Schematic structures of hATF6α, hATF6α(C)-TAP, hATF6α(C)-myct, and its three deletion mutants. bZIP and TMD denote basic leucine zipper and transmembrane domains, respectively. N indicates a potential glycosylation site. Both the amino acids 111–119 and 182–194 are expected to form an α-helix. (B) Immunoblotting of cell lysates prepared from WT and gEDEM-TKO cells expressing one of the four hATF6α(C) derivatives by transfection with or without EndoH treatment using anti–c-myc. (C–F) Cycloheximide chase of WT and gEDEM-TKO cells expressing one of the four hATF6α(C) derivatives by transfection using anti–c-myc (n = 3). Means ± SD are shown. *, P < 0.05; **, P < 0.01.

mutants were more misfolded than hATF6α(C)-myct1-302 and Δ280–298 mutant (Fig. S3 F).

To substantiate our hypothesis further, we determined whether severely misfolded glycoproteins are degraded by non-gpERAD in human cells also. For this, we focused on mouse CD3-δ-ΔTM, an ERAD-Ls substrate containing three potential N-glycosylation sites (Fig. 4 A; Bernasconi et al., 2010), which is localized in the ER (Fig. 4 B), because a part of hATF6α(C)-myct1-302 was secreted into medium in HCT116 cells (not depicted), contrary to its full retention in the ER of DT40 cells. The results of the PNGase sensitivity assay in cell lysates suggested that the two insertion mutants were more misfolded than WT (Fig. 4 C). We found that degradation of exogenously expressed mCD3-δ-ΔTM was delayed in hEDEM-TKO cells (Fig. 4 D) to a similar extent to that in WT cells treated with MG132 (Fig. 4 E) or kifunensine (not depicted). Importantly, insertion of 7 aa (Pro-Ala-Pro-Ala-Pro-Ala-Pro) between 33 and 34 aa (mCD3-δ-ΔTM<33-7aa-34>) or 70 and 71 aa (mCD3-δ-ΔTM<70-7aa-71>), present in the second or sixth β-sheet, respectively, in the case of human CD3-δ (Fig. S3 G) resulted in similar degradation of the mutant proteins in the two types of cells, except for a delay at the early chase period in hEDEM-TKO cells (Fig. 4 F), despite their localization in the ER (Fig. 4 B).

We further found that the type I transmembrane human protein EMC1 containing three potential N-glycosylation sites (Fig. 5 A), a subunit of the ER membrane protein complex consisting of six subunits (EMC1–EMC6; Jonikas et al., 2009), behaved like ATF6α. Endogenous hEMC1 turned over slowly in WT HCT116 cells, and its turnover was delayed in hEDEM-TKO cells (Fig. 5 B). Exogenously expressed Flag-tagged hEMC1 was localized in the ER (Fig. 5 C) and behaved very similarly to endogenous hEMC1 (Fig. 5 E). Importantly, however, its Δ35–220 mutant, which lacks most of the pyrroloquinoline quinone (PQQ) domain

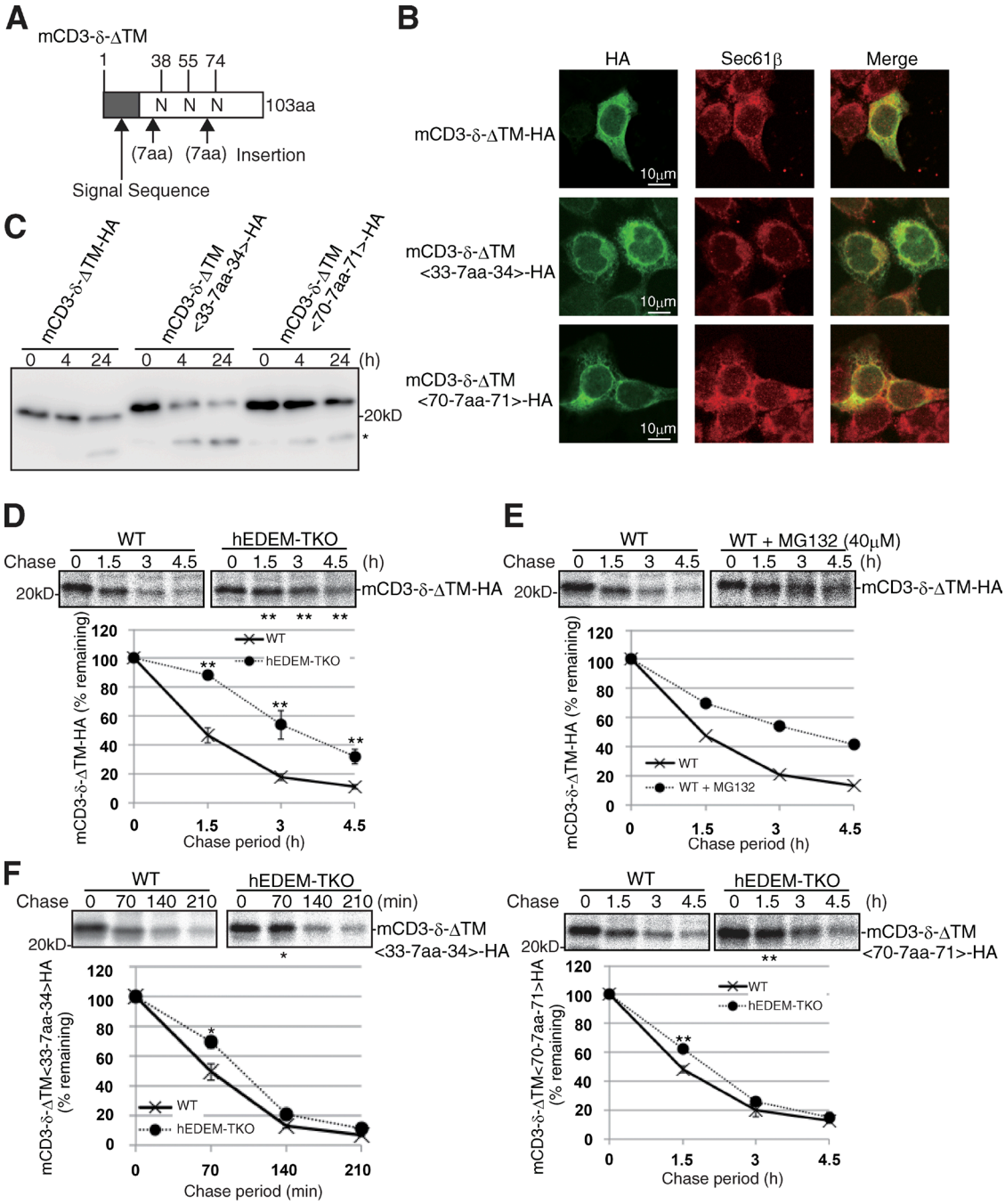

Figure 4. **Effect of EDEM-TKO on mCD3-δ–ΔTM degradation.** (A) Schematic structures of WT and two insertion mutants of mCD3-δ–ΔTM. (B) Immunofluorescence of HCT116 cells expressing transfected WT or insertion mutant of mCD3-δ–ΔTM using anti-HA. (C) PNGase sensitivity assay of WT and two insertion mutants of mCD3-δ–ΔTM expressed in HCT116 cells by transfection (immunoblotting with anti-HA). The asterisk denotes partially deglycosylated mCD3-δ–ΔTM. (D) Pulse-chase to determine the degradation rate of transfected WT mCD3-δ–ΔTM in WT and hEDEM-TKO cells using anti-HA (n = 3). (E) Pulse-chase to determine the degradation rate of transfected WT mCD3-δ–ΔTM in WT cells and those treated with 40 μM MG132 using anti-HA. This experiment was completed once. (F) Pulse-chase to determine the degradation rate of transfected insertion mutants of mCD3-δ–ΔTM in WT and hEDEM-TKO cells using anti-HA (n = 3). (D–F) Means ± SD are shown. (D and F) *, $P < 0.05$; **, $P < 0.01$.

containing the β-propeller repeat (Kopec and Lupas, 2013), was localized in the ER (Fig. 5 C), was more sensitive to trypsin and therefore more misfolded than hEMC1-Flag (Fig. 5 D), and was degraded similarly in the two types of cells, except for a delay at the early chase period in hEDEM-TKO cells (Fig. 5 E).

Our results identified a previously unnoticed system operating in the ER. Chicken and human cells can degrade severely misfolded glycoproteins in the absence of EDEM-mediated mannose trimming. This novel quality control cannot be easily discerned by knocking down EDEM1/2/3 singularly, and was accordingly identified for the first time here after our construction of EDEM-TKO cells in combination with our comparison of the fates of ATF6α and NHK. Based on the results reported for recombinant human ERmanI (Aikawa et al., 2012), we consider that ERmanI cannot trim $Man_9GlcNAc_2$ present in native but unstable or somewhat unfolded glycoproteins, leading

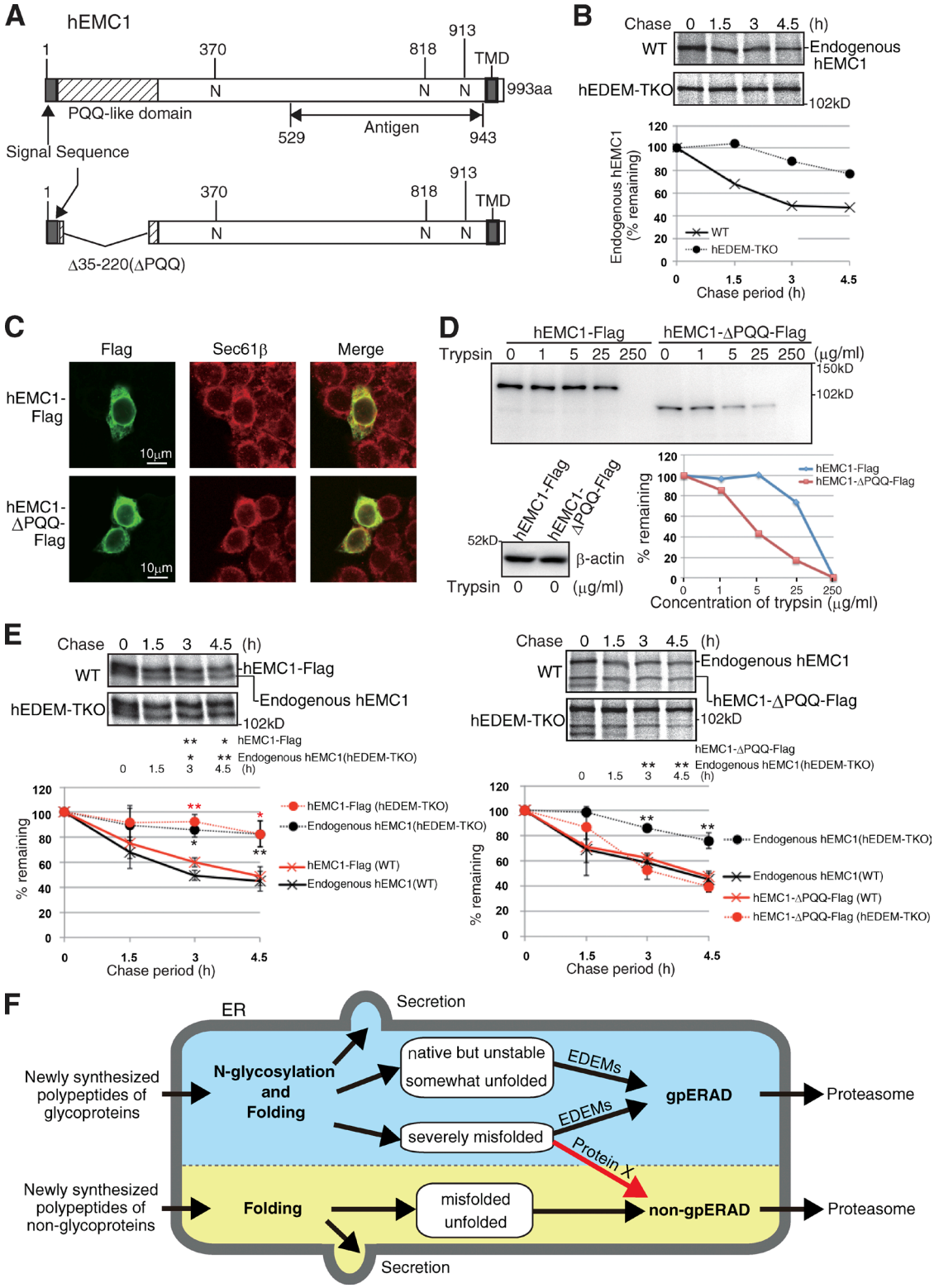

Figure 5. **Effect of EDEM-TKO on hEMC1 degradation.** (A) Schematic structures of WT and deletion mutant of hEMC1. (B) Pulse-chase to determine the degradation rate of endogenous hEMC1 in WT and hEDEM-TKO cells using anti-hEMC1. This experiment was completed once. (C) Immunofluorescence of HCT116 cells expressing transfected hEMC1-Flag or hEMC1-ΔPQQ-Flag using anti-Flag. (D) Trypsin sensitivity assay of hEMC1-Flag and hEMC1-ΔPQQ-Flag expressed in HCT116 cells by transfection (immunoblotting with anti-Flag). The data shown are from a single representative experiment out of two repeats. (E) Pulse-chase to determine the degradation rate of transfected hEMC1-Flag and hEMC1-ΔPQQ-Flag, as well as endogenous hEMC1 in WT and hEDEM-TKO cells using anti-hEMC1 ($n = 3$). Means ± SD are shown. *, $P < 0.05$; **, $P < 0.01$. (F) Model. Newly synthesized polypeptides of non-glycoproteins are subjected to productive folding. Folded non-glycoproteins are secreted, whereas unfolded or misfolded proteins are targeted to non-gpERAD for proteasomal degradation. Newly synthesized polypeptides of glycoproteins are subjected to N-glycosylation and productive folding. Folded glycoproteins are secreted, whereas native but unstable glycoproteins, somewhat unfolded glycoproteins, and severely misfolded glycoproteins are subjected to EDEM-mediated mannose trimming, followed by proteasomal degradation via gpERAD. In addition, severely misfolded glycoproteins are subjected to non-gpERAD via protein X.

to marked stabilization of ATF6α in EDEM2 single KO cells (Ninagawa et al., 2014), but can trim $Man_9GlcNAc_2$ present in severely misfolded glycoproteins, such as NHK, to produce $Man_8GlcNAc_2$ in EDEM2 single KO cells, which is trimmed to $Man_7GlcNAc_2$ by EDEM3/1 for proteasomal degradation (Fig. 2 F). Indeed, degradation of NHK was markedly blocked by kifunensine, which inhibits both ERmanI and EDEM1/2/3, at the early chase period (1.5 h) in HCT116 cells (Fig. 2, G and H). This also explains the apparent blockade of NHK degradation by kifunensine observed at the early chase periods (1–2 h) in previous studies (Hosokawa et al., 2001; Hirao et al., 2006). Complete blockade at 3-h chase (Liu et al., 1999) was not reproduced in either recent studies (Pan et al., 2011; Fujimori et al., 2013) or here (Fig. 2, G and H).

This protein structure–based decision is made only in higher eukaryotes because yeast does not possess an efficient non-gpERAD (Jakob et al., 2001; Kostova and Wolf, 2005). In marked contrast, degradation of NHK-QQQ is much more efficient than that of NHK in both mammalian (Hosokawa et al., 2008) and DT40 cells (compare Fig. 2 B with Fig. 2 D). This explains why the delay in NHK degradation at the early chase periods in EDEM-TKO cells was canceled in the later chase periods (Fig. 2, D and G).

The next obvious question is what molecules extract severely misfolded glycoproteins from gpERAD and target them to non-gpERAD (protein X in Fig. 5 F). Identification of the switch will further enhance our understanding of the protein quality control operating in the ER.

Materials and methods

Construction of plasmids

Recombinant DNA techniques were performed according to standard procedures (Sambrook et al., 1989). The integrity of all constructed plasmids was confirmed by extensive sequencing analyses. Site-directed mutagenesis was performed using Dpn I. p3*flag-CMV-14 Expression Vector (Sigma-Aldrich) was used to express a protein tagged with Flag at the C terminus. Platinum transcription activator-like effector nuclease plasmids to knock out hEDEM family genes were constructed previously (Ninagawa et al., 2014).

Reagents

Puromycin (0.5 µg/ml), histidinol (1 mg/ml), mycophenolic acid (15 µg/ml), blasticidin S (25 µg/ml), G418 (2 mg/ml for DT40 and 0.6 mg/ml for HCT116), and Zeocin (1 mg/ml) were used for the selection and maintenance of drug-resistant clones. Kifunensine was purchased from Cayman Chemical Company, EndoH from EMD Millipore, cycloheximide from Sigma-Aldrich, MG132 from Peptide Institute, Z-VAD-fmk from Promega, trypsin from Nacalai Tesque, and digitonin from Wako Pure Chemical Industries.

Cell culture, transfection, and N-glycan profiling

DT40 cells were cultured and transfected as described previously (Ninagawa et al., 2011). HCT116 cells (ATCC CCL-247) and MEF cells were cultured in Dulbecco's modified Eagle's medium (glucose 4.5 g/liter) supplemented with 10% fetal bovine serum, 2 mM glutamine, and antibiotics (100 U/ml penicillin and 100 µg/ml streptomycin) at 37°C in a humidified 5% CO_2/95% air atmosphere and transfected using Lipofectamine 2000 (Invitrogen) or X-tremeGENE 9 (Roche) according to the manufacturers' instructions. Doubling times were determined by counting cell numbers every 24 h for a total of 120 h for DT40 cells, and every 48 h for a total of 192 h for HCT116 cells. Each value represents the mean of triplicate determinations. Pyridylamination and structural identification of N-glycans of total cellular glycoproteins were performed as described previously (Horimoto et al., 2013; Ninagawa et al., 2014).

Immunological techniques

Immunoblotting analysis was performed according to the standard procedure (Sambrook et al., 1989) as described previously (Ninagawa et al., 2011). Chemiluminescence obtained using Western Blotting Luminol Reagent (Santa Cruz Biotechnology, Inc.) was detected using an LAS-3000mini Lumino Image analyzer (Fujifilm). Rabbit anti–chicken ATF6 (Horimoto et al., 2013) and anti–human ATF6α (Haze et al., 1999) antibodies were raised previously. Rabbit polyclonal anti-EMC1 antibody, which reacts with both chicken and human EMC1, was raised against human EMC1 (529–943 aa) fused to glutathione *S*-transferase. Anti–c-myc antibody (9E10) was obtained from Wako Pure Chemical Industries, anti-Flag antibody from Sigma-Aldrich, anti-HA antibody from Recenttec, anti-KDEL antibody from Medical and Biological Laboratories, anti-ATF4 and anti-XBP1 antibodies from Santa Cruz Biotechnology, Inc., and anti-α1PI antibody from Dako.

Pulse-chase experiments using 9.8 MBq/dish EASY TAG EXPRESS Protein labeling mix [^{35}S] (PerkinElmer) and subsequent immunoprecipitation using anti–human ATF6α, anti-α1PI, anti–human EMC1, anti-Flag, or anti-HA antibody and protein A–coupled Sepharose beads (GE Healthcare) were performed according to procedures described previously (Ninagawa et al., 2011).

For immunofluorescence analysis, HCT116 cells transfected using X-tremeGENE 9 were fixed by incubation on ice for 6.5 min in methanol/acetone (1:1). Anti-Sec61β antibody was obtained from Proteintech. Secondary antibodies labeled with FITC and CF594 were obtained from ICN Biomedicals and Biotium, respectively. Microscope images were obtained at room temperature with 40 magnification using a DM IRE2 and confocal software (both from Leica).

PNGase sensitivity assay

HCT116 cells at 24 h after transfection or DT40 cells at 16 h after transfection were washed with PBS, collected, and suspended in 200 µl buffer A (50 mM Tris/HCl, pH 8.0, containing 1% NP-40 [for mammalian cells] or 1% digitonin [for chicken cells], 150 mM NaCl, protease inhibitor cocktail [Nacalai Tesque], and 20 µM MG132). Lysates were left on ice for 20 min and clarified by centrifugation at 14,000 rpm for 10 min at 4°C. After incubation for various periods on ice, cleared lysates were mixed with 2× SDS sample buffer containing 100 mM dithiothreitol and 2 µM Z-VAD-fmk, boiled for 5 min, and subjected to SDS-PAGE followed by immunoblotting.

Trypsin sensitivity assay

DT40 cells or HCT116 cells transfected were washed with PBS three times, collected, and suspended in 250 µl (for DT40 cells) or 400 µl (for HCT116 cells) buffer B (50 mM Tris/HCl, pH 8.0, containing 1% NP-40, 150 mM NaCl, 2 µM Z-VAD-fmk, and 20 µM MG132). Lysates were left on ice for 20 min and clarified by centrifugation at 14,000 rpm for 10 min at 4°C. Cleared lysates were incubated with various concentrations of trypsin for 15 min at 4°C and then mixed with 2× SDS sample buffer containing 100 mM dithiothreitol and 10× protease inhibitor cocktail (Nacalai Tesque), boiled for 5 min, and subjected to SDS-PAGE followed by immunoblotting. The presence of equal amounts of proteins in cleared lysates before trypsin digestion was confirmed by immunoblotting with anti–β-actin antibody.

Southern blot hybridization

Southern blot hybridization was performed according to standard procedures (Sambrook et al., 1989) as described previously (Ninagawa et al., 2011). Specific probes were prepared as described previously (Ninagawa et al., 2014) and labeled with digoxigenin. Subsequent reaction with anti-digoxigenin antibody (Roche) and treatment with the chemiluminescent detection reagent CDP-star (GE Healthcare) were performed according to the manufacturers' specifications. Chemiluminescence was visualized using an LAS-3000mini Lumino Image analyzer (Fujifilm).

Genomic PCR

Homologous recombination in HCT116 cells was confirmed by genomic PCR using a pair of primers described previously (Ninagawa et al., 2014).

RT-PCR

Total RNA prepared from WT DT40 cells or various KOs (~5 × 10^6 cells) and from WT HCT116 cells or various KOs (~3 × 10^6 cells) by the acid guanidinium/phenol/chloroform method using ISOGEN (Nippon Gene) was converted to cDNA using Moloney murine leukemia virus reverse transcription (Invitrogen) and random primers. The full-length open reading frame of gEDEM1, gEDEM2, gEDEM3, hEDEM1, hEDEM2, or hEDEM3 was amplified using PrimeSTAR HS DNA polymerase (Takara Bio Inc.) and a pair of primers described previously (Ninagawa et al., 2014).

Construction of gEDEM-TKO DT40 cells

We previously constructed gEDEM1, gEDEM2, or gEDEM3 single KO DT40 cells (Ninagawa et al., 2014). We then constructed double KO cells deficient in gEDEM1 and gEDEM2, gEDEM2 and gEDEM3, and gEDEM1 and gEDEM3 (Fig. S1 A). Homologous recombination was checked by Southern blotting (Fig. S1 B), and RT-PCR analysis revealed the expected expression of each mRNA (Fig. S1 C). We further constructed TKO cells deficient in gEDEM1, gEDEM2, and gEDEM3 (Fig. S1 A, right). Homologous recombination was checked by Southern blotting (Fig. S1 B), and RT-PCR analysis revealed the expected expression of each mRNA (Fig. S1 C).

Construction of hEDEM-TKO HCT116 cells

We previously constructed hEDEM1, hEDEM2, or hEDEM3 single KO HCT116 cells (Ninagawa et al., 2014). We disrupted the hEDEM2 gene in hEDEM3 single KO cells and then disrupted the hEDEM1 gene in the resulting hEDEM2/3 double KO cells to create hEDEM-TKO HCT116 cells (Fig. S2 A).

Online supplemental material

Fig. S1 shows the generation of DT40 cells deficient in two or three of gEDEM1/2/3. Fig. S2 shows the generation and characterization of hEDEM-TKO cells and the effect of MG132 on the stability of hATF6α(C) derivatives in DT40 cells. Fig. S3 shows analysis of folding status of hATF6α(C) derivatives in DT40 cells. Online supplemental material is available at http://www.jcb.org/cgi/content/full/jcb.201504109/DC1. Additional data are available in the JCB DataViewer at http://dx.doi.org/10.1083/jcb.201504109.dv.

Acknowledgments

We thank Ms. Kaoru Miyagawa for her technical and secretarial assistance and Ms. Yukiko Isono (IMS) for her help in the analyses of N-glycans. We are grateful to people in the Yamate-Area Facility, Center for Radioisotope Facilities, and Okazaki Research Facilities, National Institutes of Natural Science.

This work was financially supported in part by grants from the Ministry of Education, Culture, Sports, Science and Technology of Japan (26291040 to K. Mori, 26840065 to S. Ninagawa, 23221005 and 15K06996 to T. Okada, 15K18529 to T. Ishikawa, 26110725 to T. Suzuki, 26102518 to Y. Kamiya, and 24249002, 25102008, and 15H02491 to K. Kato) and by the Joint Studies Program (2014-2015) of the Institute for Molecular Science.

The authors declare no competing financial interests.

Submitted: 24 April 2015
Accepted: 7 October 2015

References

Aikawa, J., I. Matsuo, and Y. Ito. 2012. In vitro mannose trimming property of human ER α-1,2 mannosidase I. *Glycoconj. J.* 29:35–45. http://dx.doi.org/10.1007/s10719-011-9362-1

Bernasconi, R., C. Galli, V. Calanca, T. Nakajima, and M. Molinari. 2010. Stringent requirement for HRD1, SEL1L, and OS-9/XTP3-B for disposal of ERAD-LS substrates. *J. Cell Biol.* 188:223–235. http://dx.doi.org/10.1083/jcb.200910042

Brodsky, J.L. 2012. Cleaning up: ER-associated degradation to the rescue. *Cell.* 151:1163–1167. http://dx.doi.org/10.1016/j.cell.2012.11.012

Fujimori, T., Y. Kamiya, K. Nagata, K. Kato, and N. Hosokawa. 2013. Endoplasmic reticulum lectin XTP3-B inhibits endoplasmic reticulum-associated degradation of a misfolded α1-antitrypsin variant. *FEBS J.* 280:1563–1575. http://dx.doi.org/10.1111/febs.12157

Haze, K., H. Yoshida, H. Yanagi, T. Yura, and K. Mori. 1999. Mammalian transcription factor ATF6 is synthesized as a transmembrane protein and activated by proteolysis in response to endoplasmic reticulum stress. *Mol. Biol. Cell.* 10:3787–3799. http://dx.doi.org/10.1091/mbc.10.11.3787

Hirao, K., Y. Natsuka, T. Tamura, I. Wada, D. Morito, S. Natsuka, P. Romero, B. Sleno, L.O. Tremblay, A. Herscovics, et al. 2006. EDEM3, a soluble EDEM homolog, enhances glycoprotein endoplasmic reticulum-associated degradation and mannose trimming. *J. Biol. Chem.* 281:9650–9658. http://dx.doi.org/10.1074/jbc.M512191200

Horimoto, S., S. Ninagawa, T. Okada, H. Koba, T. Sugimoto, Y. Kamiya, K. Kato, S. Takeda, and K. Mori. 2013. The unfolded protein response transducer ATF6 represents a novel transmembrane-type endoplasmic reticulum-associated degradation substrate requiring both mannose trimming and SEL1L protein. *J. Biol. Chem.* 288:31517–31527. http://dx.doi.org/10.1074/jbc.M113.476010

Hosokawa, N., I. Wada, K. Hasegawa, T. Yorihuzi, L.O. Tremblay, A. Herscovics, and K. Nagata. 2001. A novel ER α-mannosidase-like protein accelerates ER-associated degradation. *EMBO Rep.* 2:415–422. http://dx.doi.org/10.1093/embo-reports/kve084

Hosokawa, N., I. Wada, K. Nagasawa, T. Moriyama, K. Okawa, and K. Nagata. 2008. Human XTP3-B forms an endoplasmic reticulum quality control scaffold with the HRD1-SEL1L ubiquitin ligase complex and BiP. *J. Biol. Chem.* 283:20914–20924. http://dx.doi.org/10.1074/jbc.M709336200

Hosokawa, N., Y. Kamiya, and K. Kato. 2010. The role of MRH domain-containing lectins in ERAD. *Glycobiology.* 20:651–660. http://dx.doi.org/10.1093/glycob/cwq013

Huang, C., Y. Harada, A. Hosomi, Y. Masahara-Negishi, J. Seino, H. Fujihira, Y. Funakoshi, T. Suzuki, N. Dohmae, and T. Suzuki. 2015. Endo-β-*N*-acetylglucosaminidase forms *N*-GlcNAc protein aggregates during ER-associated degradation in Ngly1-defective cells. *Proc. Natl. Acad. Sci. USA.* 112:1398–1403. http://dx.doi.org/10.1073/pnas.1414593112

Izawa, T., H. Nagai, T. Endo, and S. Nishikawa. 2012. Yos9p and Hrd1p mediate ER retention of misfolded proteins for ER-associated degradation. *Mol. Biol. Cell.* 23:1283–1293. http://dx.doi.org/10.1091/mbc.E11-08-0722

Jakob, C.A., D. Bodmer, U. Spirig, P. Battig, A. Marcil, D. Dignard, J.J. Bergeron, D.Y. Thomas, and M. Aebi. 2001. Htm1p, a mannosidase-like protein, is involved in glycoprotein degradation in yeast. *EMBO Rep.* 2:423–430. http://dx.doi.org/10.1093/embo-reports/kve089

Jonikas, M.C., S.R. Collins, V. Denic, E. Oh, E.M. Quan, V. Schmid, J. Weibezahn, B. Schwappach, P. Walter, J.S. Weissman, and M. Schuldiner. 2009. Comprehensive characterization of genes required for protein folding in the endoplasmic reticulum. *Science.* 323:1693–1697. http://dx.doi.org/10.1126/science.1167983

Kamiya, Y., T. Satoh, and K. Kato. 2012. Molecular and structural basis for N-glycan-dependent determination of glycoprotein fates in cells.

Biochim. Biophys. Acta. 1820:1327–1337. http://dx.doi.org/10.1016/j.bbagen.2011.12.017

Kopec, K.O., and A.N. Lupas. 2013. β-Propeller blades as ancestral peptides in protein evolution. *PLoS One.* 8:e77074. (published erratum appears in *PLoS One*. 2014. 9. http://dx.doi.org/10.1371/annotation/fee01544-ff98-4ed2-9dc9-7aea9c5fe828) http://dx.doi.org/10.1371/journal.pone.0077074

Kostova, Z., and D.H. Wolf. 2005. Importance of carbohydrate positioning in the recognition of mutated CPY for ER-associated degradation. *J. Cell Sci.* 118:1485–1492. http://dx.doi.org/10.1242/jcs.01740

Liu, Y., P. Choudhury, C.M. Cabral, and R.N. Sifers. 1999. Oligosaccharide modification in the early secretory pathway directs the selection of a misfolded glycoprotein for degradation by the proteasome. *J. Biol. Chem.* 274:5861–5867. http://dx.doi.org/10.1074/jbc.274.9.5861

Mast, S.W., K. Diekman, K. Karaveg, A. Davis, R.N. Sifers, and K.W. Moremen. 2005. Human EDEM2, a novel homolog of family 47 glycosidases, is involved in ER-associated degradation of glycoproteins. *Glycobiology.* 15:421–436. http://dx.doi.org/10.1093/glycob/cwi014

Misaghi, S., M.E. Pacold, D. Blom, H.L. Ploegh, and G.A. Korbel. 2004. Using a small molecule inhibitor of peptide: N-glycanase to probe its role in glycoprotein turnover. *Chem. Biol.* 11:1677–1687. http://dx.doi.org/10.1016/j.chembiol.2004.11.010

Molinari, M. 2007. N-glycan structure dictates extension of protein folding or onset of disposal. *Nat. Chem. Biol.* 3:313–320. http://dx.doi.org/10.1038/nchembio880

Ninagawa, S., T. Okada, S. Takeda, and K. Mori. 2011. SEL1L is required for endoplasmic reticulum-associated degradation of misfolded luminal proteins but not transmembrane proteins in chicken DT40 cell line. *Cell Struct. Funct.* 36:187–195. http://dx.doi.org/10.1247/csf.11018

Ninagawa, S., T. Okada, Y. Sumitomo, Y. Kamiya, K. Kato, S. Horimoto, T. Ishikawa, S. Takeda, T. Sakuma, T. Yamamoto, and K. Mori. 2014. EDEM2 initiates mammalian glycoprotein ERAD by catalyzing the first mannose trimming step. *J. Cell Biol.* 206:347–356. http://dx.doi.org/10.1083/jcb.201404075

Pan, S., S. Wang, B. Utama, L. Huang, N. Blok, M.K. Estes, K.W. Moremen, and R.N. Sifers. 2011. Golgi localization of ERManI defines spatial separation of the mammalian glycoprotein quality control system. *Mol. Biol. Cell.* 22:2810–2822. http://dx.doi.org/10.1091/mbc.E11-02-0118

Rosenbaum, J.C., E.K. Fredrickson, M.L. Oeser, C.M. Garrett-Engele, M.N. Locke, L.A. Richardson, Z.W. Nelson, E.D. Hetrick, T.I. Milac, D.E. Gottschling, and R.G. Gardner. 2011. Disorder targets misorder in nuclear quality control degradation: a disordered ubiquitin ligase directly recognizes its misfolded substrates. *Mol. Cell.* 41:93–106. http://dx.doi.org/10.1016/j.molcel.2010.12.004

Sambrook, J., E.F. Fritsch, and T. Maniatis. 1989. Molecular Cloning: A Laboratory Manual. Cold Spring Harbor Laboratory Press, Cold Spring Harbor, New York. 1626 pp.

Sifers, R.N., S. Brashears-Macatee, V.J. Kidd, H. Muensch, and S.L. Woo. 1988. A frameshift mutation results in a truncated alpha 1-antitrypsin that is retained within the rough endoplasmic reticulum. *J. Biol. Chem.* 263:7330–7335.

Smith, M.H., H.L. Ploegh, and J.S. Weissman. 2011. Road to ruin: targeting proteins for degradation in the endoplasmic reticulum. *Science.* 334:1086–1090. http://dx.doi.org/10.1126/science.1209235

Ushioda, R., J. Hoseki, and K. Nagata. 2013. Glycosylation-independent ERAD pathway serves as a backup system under ER stress. *Mol. Biol. Cell.* 24:3155–3163. http://dx.doi.org/10.1091/mbc.E13-03-0138

Xie, W., and D.T. Ng. 2010. ERAD substrate recognition in budding yeast. *Semin. Cell Dev. Biol.* 21:533–539. http://dx.doi.org/10.1016/j.semcdb.2010.02.007

Xu, C., S. Wang, G. Thibault, and D.T. Ng. 2013. Futile protein folding cycles in the ER are terminated by the unfolded protein O-mannosylation pathway. *Science.* 340:978–981. http://dx.doi.org/10.1126/science.1234055